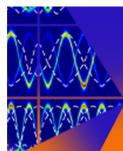# Shock compression experiments using the DiPOLE 100-X laser on the high energy density instrument at the European x-ray free electron laser: Quantitative structural analysis of liquid Sn ⊚ ⓕ

M. G. Gorman ✉ ⓘ ; D. McGonegle ⓘ ; R. F. Smith ⓘ ; S. Singh ⓘ ; T. Jenkins ⓘ ; R. S. McWilliams ⓘ ;
B. Albertazzi; S. J. Ali ⓘ ; L. Antonelli ⓘ ; M. R. Armstrong ⓘ ; C. Baehtz ⓘ ; O. B. Ball ⓘ ; S. Banerjee ⓘ ;
A. B. Belonoshko; A. Benuzzi-Mounaix; C. A. Bolme ⓘ ; V. Bouffetier; R. Briggs ⓘ ; K. Buakor ⓘ ; T. Butcher;
S. Di Dio Cafiso; V. Cerantola; J. Chantel ⓘ ; A. Di Cicco ⓘ ; S. Clarke ⓘ ; A. L. Coleman ⓘ ; J. Collier ⓘ ;
G. W. Collins ⓘ ; A. J. Comley ⓘ ; F. Coppari ⓘ ; T. E. Cowan ; G. Cristoforetti ⓘ ; H. Cynn ⓘ ;
A. Descamps ⓘ ; F. Dorchies ⓘ ; M. J. Duff; A. Dwivedi; C. Edwards; J. H. Eggert ⓘ ; D. Errandonea ⓘ ;
G. Fiquet ⓘ ; E. Galtier ⓘ ; A. Laso Garcia ⓘ ; H. Ginestet ⓘ ; L. Gizzi; A. Gleason ⓘ ; S. Goede;
J. M. Gonzalez ⓘ ; M. Harmand ⓘ ; N. J. Hartley ⓘ ; P. G. Heighway ⓘ ; C. Hernandez-Gomez ⓘ ;
A. Higginbotham ⓘ ; H. Höppner ⓘ ; R. J. Husband ⓘ ; T. M. Hutchinson ⓘ ; H. Hwang; A. E. Lazicki ⓘ ;
D. A. Keen ⓘ ; J. Kim ⓘ ; P. Koester ⓘ ; Z. Konopkova ⓘ ; D. Kraus ⓘ ; A. Krygier ⓘ ; L. Labate ⓘ ; Y. Lee ⓘ ;
H.-P. Liermann ⓘ ; P. Mason ⓘ ; M. Masruri ⓘ ; B. Massani; E. E. McBride ⓘ ; C. McGuire; J. D. McHardy ⓘ ;
S. Merkel ⓘ ; G. Morard ⓘ ; B. Nagler ⓘ ; M. Nakatsutsumi ⓘ ; K. Nguyen-Cong ⓘ ; A.-M. Norton ⓘ ;
I. I. Oleynik ⓘ ; C. Otzen ⓘ ; N. Ozaki ⓘ ; S. Pandolfi ⓘ ; D. J. Peake; A. Pelka; K. A. Pereira; J. P. Phillips ⓘ ;
C. Prescher ⓘ ; T. R. Preston ⓘ ; L. Randolph ⓘ ; D. Ranjan ⓘ ; A. Ravasio; R. Redmer ⓘ ; J. Rips ⓘ ;
D. Santamaria-Perez ⓘ ; D. J. Savage ⓘ ; M. Schoelmerich; J.-P. Schwinkendorf ⓘ ; J. Smith ; A. Sollier ⓘ ;
J. Spear; C. Spindloe ⓘ ; M. Stevenson ⓘ ; C. Strohm ⓘ ; T.-A. Suer; M. Tang; M. Toncian ⓘ ; T. Toncian ⓘ ;
S. J. Tracy; A. Trapananti ⓘ ; T. Tschentscher ⓘ ; M. Tyldesley; C. E. Vennari; T. Vinci ⓘ ; S. C. Vogel ⓘ ;
T. J. Volz ⓘ ; J. Vorberger ⓘ ; J. P. S. Walsh ⓘ ; J. S. Wark ⓘ ; J. T. Willman; L. Wollenweber ⓘ ; U. Zastrau ⓘ ;
E. Brambrink ⓘ ; K. Appel ⓘ ; M. I. McMahon ⓘ

Check for updates

View Online

Export Citation

07 June 2024 15:19:42

Journal of Applied Physics

Special Topic:
Thermal Transport in 2D Materials

Submit Today

AIP Publishing

Shock compression experiments using the DiPOLE 100-X laser on the high energy density instrument at the European x-ray free electron laser: Quantitative structural analysis of liquid Sn

M. G. Gorman,[1,a] D. McGonegle,[2] R. F. Smith,[1] S. Singh,[1] T. Jenkins,[3] R. S. McWilliams,[3] B. Albertazzi,[4] S. J. Ali,[1] L. Antonelli,[5] M. R. Armstrong,[1] C. Baehtz,[6] O. B. Ball,[3] S. Banerjee,[7] A. B. Belonoshko,[8] A. Benuzzi-Mounaix,[4] C. A. Bolme,[9] V. Bouffetier,[10] R. Briggs,[1] K. Buakor,[10] T. Butcher,[7] S. Di Dio Cafiso,[6] V. Cerantola,[11] J. Chantel,[12] A. Di Cicco,[13] S. Clarke,[1] A. L. Coleman,[1] J. Collier,[7] G. W. Collins,[14] A. J. Comley,[2] F. Coppari,[1] T. E. Cowan,[6] G. Cristoforetti,[15] H. Cynn,[1] A. Descamps,[16] F. Dorchies,[17] M. J. Duff,[3] A. Dwivedi,[10] C. Edwards,[7] J. H. Eggert,[1] D. Errandonea,[18] G. Fiquet,[19] E. Galtier,[20] A. Laso Garcia,[6] H. Ginestet,[12] L. Gizzi,[21] A. Gleason,[20] S. Goede,[10] J. M. Gonzalez,[22] M. Harmand,[19,23] N. J. Hartley,[20] P. G. Heighway,[24] C. Hernandez-Gomez,[7] A. Higginbotham,[5] H. Höppner,[6] R. J. Husband,[25] T. M. Hutchinson,[1] H. Hwang,[25] A. E. Lazicki,[1] D. A. Keen,[26] J. Kim,[27] P. Koester,[15] Z. Konopkova,[10] D. Kraus,[6,28] A. Krygier,[1] L. Labate,[15] Y. Lee,[29] H.-P. Liermann,[25] P. Mason,[7] M. Masruri,[6] B. Massani,[3] E. E. McBride,[16] C. McGuire,[1] J. D. McHardy,[3] S. Merkel,[12] G. Morard,[30] B. Nagler,[20] M. Nakatsutsumi,[10] K. Nguyen-Cong,[22] A.-M. Norton,[5] I. I. Oleynik,[22] C. Otzen,[31] N. Ozaki,[32] S. Pandolfi,[19] D. J. Peake,[24] A. Pelka,[6] K. A. Pereira,[33] J. P. Phillips,[7] C. Prescher,[31] T. R. Preston,[10] L. Randolph,[10] D. Ranjan,[6,28] A. Ravasio,[4] R. Redmer,[28] J. Rips,[28] D. Santamaria-Perez,[18] D. J. Savage,[9] M. Schoelmerich,[34] J.-P. Schwinkendorf,[6] J. Smith,[7] A. Sollier,[35,36] J. Spear,[7] C. Spindloe,[7] M. Stevenson,[28] C. Strohm,[25] T.-A. Suer,[14] M. Tang,[25] M. Toncian,[6] T. Toncian,[6] S. J. Tracy,[37] A. Trapananti,[13] T. Tschentscher,[10] M. Tyldesley,[7] C. E. Vennari,[1] T. Vinci,[4] S. C. Vogel,[9] T. J. Volz,[1] J. Vorberger,[6] J. P. S. Walsh,[33] J. S. Wark,[24] J. T. Willman,[22] L. Wollenweber,[10] U. Zastrau,[10] E. Brambrink,[10] K. Appel,[10] and M. I. McMahon[3]

AFFILIATIONS

[1]Lawrence Livermore National Laboratory, Livermore, California 94550, USA
[2]Atomic Weapons Establishment (AWE), Aldermaston, Reading, RG7 4PR, United Kingdom
[3]SUPA, School of Physics and Astronomy, and Centre for Science at Extreme Conditions, The University of Edinburgh, Edinburgh EH9 3FD, United Kingdom
[4]Ecole Polytechnique, Palaiseau, Laboratoire pour l'utilisation des lasers intenses (LULI), CNRS UMR 7605, Route de Saclay, 91128 PALAISEAU Cedex, France
[5]University of York, School of Physics, Engineering and Technology, Heslington York YO10 5DD, United Kingdom
[6]Helmholtz-Zentrum Dresden-Rossendorf (HZDR), Bautzner Landstraße 400, 01328 Dresden, Germany
[7]Central Laser Facility (CLF), STFC Rutherford Appleton Laboratory, Harwell Campus, Didcot OX11 0QX, United Kingdom
[8]Frontiers Science Center for Critical Earth Material Cycling, School of Earth Sciences and Engineering, Nanjing University, Nanjing 210023, China
[9]Los Alamos National Laboratory, Los Alamos, New Mexico 87545, USA
[10]European XFEL, Holzkoppel 4, 22869 Schenefeld, Germany

07 June 2024 15:19:42

[11]Università degli Studi di Milano Bicocca, Dipartimento di Scienze dell'Ambiente e della Terra, Piazza della Scienza 1e4, I-20126 Milano, Italy

[12]Univ. Lille, CNRS, INRAE, Centrale Lille, UMR 8207—UMET—Unité Matériaux et Transformations, F-59000 Lille, France

[13]School of Science and Technology—Physics Division, University of Camerino, 62032 Camerino, Italy

[14]University of Rochester, Laboratory for Laser Energetics (LLE), 250 East River Road, Rochester, New York 14623-1299, USA

[15]CNR - Consiglio Nazionale delle Ricerche, Istituto Nazionale di Ottica, (CNR—INO), Largo Enrico Fermi 6, 50125 Firenze FI, Italy

[16]School of Mathematics and Physics, Queen's University Belfast, University Road, Belfast BT7 1NN, United Kingdom

[17]Université de Bordeaux, CNRS, CEA, CELIA, UMR 5107, F-33400 Talence, France

[18]Universidad de Valencia—UV, Departamento de Fisica Aplicada—ICMUV, C/Dr. Moliner 50 Burjassot, E-46100 Valencia, Spain

[19]Sorbonne Université, Muséum National d'Histoire Naturelle, UMR CNRS 7590, Insitut de Minéralogie, de Physique, des Matériaux, et de Cosmochinie, IMPMC, Paris 75005, France

[20]SLAC National Accelerator Laboratory, 2575 Sand Hill Road, Menlo Park, California 94025, USA

[21]CNR—Consiglio Nazionale delle Ricerche, Istituto Nazionale di Ottica, (CNR—INO), Via G. Moruzzi 1, 56124 Pisa, Italy

[22]Department of Physics, University of South Florida, Tampa, Florida 33620, USA

[23]PIMM, Arts et Metiers Institute of Technology, CNRS, Cnam, HESAM University, 151 boulevard de l'Hopital, 75013 Paris, France

[24]Department of Physics, Clarendon Laboratory, University of Oxford, Parks Road, Oxford OX1 3PU, United Kingdom

[25]Deutsches Elektronen-Synchrotron DESY, Notkestr. 85, 22607 Hamburg, Germany

[26]ISIS Facility, STFC Rutherford Appleton Laboratory, Harwell Campus, Didcot OX11 0QX, United Kingdom

[27]Hanyang University, Department of Physics, 17 Haengdang dong, Seongdong gu Seoul 133-791, Korea, South Korea

[28]Universität Rostock, Institut für Physik, D-18051 Rostock, Germany

[29]Yonsei University, Department of Earth System Sciences, 50 Yonsei-ro Seodaemun-gu, Seoul 03722, Republic of Korea, South Korea

[30]Univ. Grenoble Alpes, Univ. Savoie Mont Blanc, CNRS, IRD, Univ. Gustave Eiffel, ISTerre, 38000 Grenoble, France

[31]Institut für Geo- und Umweltnaturwissenschaften, Albert-Ludwigs-Universität Freiburg, Hermann-Herder-Straße 5, 79104 Freiburg, Germany

[32]Osaka University, Graduate School of Engineering, 2-1 Yamada-oka, Suita, Osaka 565-0871, Japan

[33]University of Massachusetts Amherst, Department of Chemistry, 690 N Pleasant St Physical Sciences Building, Amherst, Massachusetts 01003-9303, USA

[34]Paul Scherrer Institut, Forschungsstrasse 111, 5232 Villigen, Switzerland

[35]CEA, DAM, DIF, 91297 Arpajon, France

[36]Université Paris-Saclay, CEA, Laboratoire Matière en Conditions Extrêmes, 91680 Bruyères-le-Châtel, France

[37]Carnegie Science, Earth and Planets Laboratory, 5241 Broad Branch Road, NW, Washington, DC 20015, USA

[a)]**Author to whom correspondence should be addressed:** gorman11@llnl.gov

07 June 2024 15:19:42

ABSTRACT

X-ray free electron laser (XFEL) sources coupled to high-power laser systems offer an avenue to study the structural dynamics of materials at extreme pressures and temperatures. The recent commissioning of the DiPOLE 100-X laser on the high energy density (HED) instrument at the European XFEL represents the state-of-the-art in combining x-ray diffraction with laser compression, allowing for compressed materials to be probed in unprecedented detail. Here, we report quantitative structural measurements of molten Sn compressed to 85(5) GPa and ∼3500 K. The capabilities of the HED instrument enable liquid density measurements with an uncertainty of ∼1% at conditions which are extremely challenging to reach via static compression methods. We discuss best practices for conducting liquid diffraction dynamic compression experiments and the necessary intensity corrections which allow for accurate quantitative analysis. We also provide a polyimide ablation pressure vs input laser energy for the DiPOLE 100-X drive laser which will serve future users of the HED instrument.

INTRODUCTION

The ability to probe laser-compressed samples with ultra-bright, femtosecond pulses of x rays from x- ray free electron laser (XFEL) sources has transformed our understanding of material behavior under dynamic compression. Indeed, there have been a number of striking results reported from XFEL studies in the last decade such as the observation of incommensurate host–guest phases forming on nanosecond timescales,[1,2] exotic carbon chemistry in plastics,[3,4] and the direct observation of plasticity mechanisms in Ta.[5] However, in the same time span, the number of XFEL or synchrotron studies of non-crystalline or amorphous materials has been comparatively sparse.[6–9] This is despite the fact that studying amorphous materials at high pressures using laser compression and XFELs has several advantages over performing similar experiments using static compression in the diamond anvil cell (DAC). For low-Z materials, the measured signal in static compression studies may be dominated by the large Compton scattering contribution from the opposing diamonds and so a large, pressure-dependent background must be subtracted accurately to extract the liquid scattering signal. To reach pressures beyond 200 GPa, the sample size in static compression experiments is restricted by the small (40 μm) diamond culets necessary to generate such pressures meaning data with low signal-to-noise ratios are typical. Furthermore, one also must always be conscious of the potential of sample contamination from interaction with the laser-heated diamond or pressure transmitting medium.[10]

In contrast, dynamic compression can reach high-pressure and high-temperature conditions with modest laser energy—For example, 40 J of laser energy in a 10 ns pulse is sufficient to compress most metals to approximately 100 GPa and several thousand kelvin. As the target package consists only of the sample of interest and a thin ablator with low atomic number, the x-ray background is usually negligible. In addition, since the experiment occurs on nanosecond timescales, chemical reactions of the sample do not have sufficient time to occur. Previous dynamic compression studies of liquids at XFEL and synchrotrons have reported quantitative measurements, but their accuracy has been hindered by several factors such as the use of multiple detectors which are not ideal for measuring accurate scattering intensities, limited angular coverage[6,7] or the use of a broad, asymmetric x-ray probe spectrum.[8,9,11]

The capabilities of the new HED instrument at the EuXFEL overcome these difficulties to enable high-accuracy structural determination of shock-compressed liquids. Here, we compressed elemental Sn to 85(5) GPa and ~3500 K and performed structure-factor analyses which determined a liquid density of 11.56(15) g/cm^3, in excellent agreement with previous shock compression data. We determined the coordination number of the liquid Sn to be 11.9(3), indicating behavior similar to a simple liquid of hard spheres which is in excellent agreement with quantum molecular dynamics (QMD) simulations of liquid Sn at similar conditions.

This paper is set out to aid future users of the facility as it discusses necessary detector intensity corrections for liquid diffraction analyses and laser energy-ablation pressure relations.
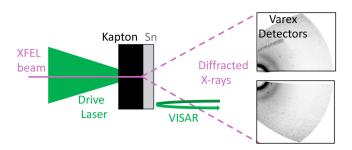

FIG. 1. Experimental setup. The target design consists of a 50 μm thick polyimide ablator bonded to a 20 μm thick Sn foil with a ~1 μm glue layer. Diffraction data from laser shock compressed Sn at an estimated pressure of 85 (5) GPa are shown. The 2D diffraction images were generated using the HEXRD diffraction software package.[13]

EXPERIMENTAL SETUP

The experiments were performed at interaction chamber 2 (IC2) at the HED instrument at the EuXFEL.[12] A schematic of the experimental setup is displayed in Fig. 1.

The DiPOLE 100-X laser,[14] which is a diode pumped ytterbium-based laser capable of up to 10 Hz operation, irradiated the sample with up to 50 J of frequency doubled (515 nm) light in a ten nanosecond pulse. The laser pulse was shaped to launch a ablatively driven shock into the sample and compress it to high pressures (Fig. 2). Phase plates were used to provide a temporally stable laser spot of diameter 500, 250, or 100 μm. The laser energy in each experiment is measured using an optic which diverts a small portion of the laser pulse to a calorimeter outside of the
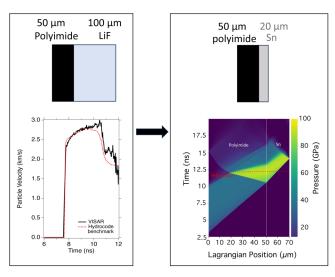

FIG. 2. Pressure determination. Experiments performed on polyimide–LiF targets are used to benchmark hydrodynamic simulations (left) which are then used to predict the pressure conditions reached in experiments which used polyimide-Sn targets at identical laser energies (right).

interaction chamber. The target package consisted of a $50\,\mu m$ poly-imide ablator which was bonded to a $20\,\mu m$ poly-crystalline Sn foil which was purchased from Goodfellow. The targets were mounted to a Al target holder which was capable of holding up to 100 targets in a 10×10 grid with 3 mm light entrance holes spaced 11 mm apart horizontally and 10 mm vertically. The EuXFEL delivered 18.0 keV x rays in a 50 fs pulse and the timing was adjusted such that the target was probed before the shock wave had exited the rear side. Two Varex 4343CT flat panel detectors were placed in a transmission geometry above and below the path of the XFEL beam which allowed for approximately 160° azimuthal coverage and angular coverage between 5° and 65° two theta. These detectors do not operate at the high vacuum within IC2 and so reside in an air-pocket located inside the interaction chamber. Each detector has a $400\,\mu m$ Al filter which preferentially absorbs lower energy x rays generated from the drive plasma relative to the higher-energy probe beam. A line-imaging Velocity Interferometer for Any Reflector (VISAR)[15] was used to monitor the rear surface velocity history of the samples in each experiment.

PRESSURE DETERMINATION

The IC2 uses a line imaging VISAR system to track the rear surface velocity of dynamically compressed samples. An optically transparent window is often bonded to the rear surface of the target to allow for determination of the particle velocity at the sample–window interface which is crucial for determining the peak sample pressure reached. As the shock wave breaks out at the sample–LiF interface, the interference fringes shift discontinuously with the magnitude of shift related to the particle velocity in the sample. The apparent velocity measured from the VISAR must be corrected for the refractive index of LiF which is non-linear as a function of pressure.[16] Two independent VISAR legs with different velocity sensitivities are employed to remove ambiguities in determining the correct sample/LiF velocity, and impedance matching between the sample and LiF is used to determine the sample particle velocity, and pressure state; the latter based on the known sample equation of state.[17]

For the Sn experiments discussed here, no confining LiF window was used and therefore the particle velocity was not measured in each experiment. This choice of target design was made to avoid any scattering from the LiF window from potentially affecting the measured liquid diffraction from the Sn sample. However, the VISAR diagnostic was able to provide accurate timing of shock break-out for the Sn experiments which allows one to determine if the sample was probed by the x rays when on compression or after pressure release. The liquid diffraction data collected in the experiments reported here were all on compression.

To determine the conditions reached by the Sn samples, we performed 1D hydrodynamic simulations[18] which were bench marked by additional experiments which used polyimide-LiF targets to accurately determined the pressure history of the polyimide ablator (Fig. 2). When agreement was reached between the experimental VISAR and the polyimide-LiF hydrodynamic simulations (Fig. 2, left), a further simulation was then performed—using the established pressure history within the polyimide—with a polyimide-Sn target to determine the pressure history in the Sn sample (Fig. 2, right). We used SESAME table 7770 for polyimide,

SESAME table number 2162 for Sn and SESAME table 7270 for LiF. Given the stability of the DiPOLE 100-X laser (the pulse shape variance shot-to-shot was negligible) and the well constrained equations of state of polyimide and Sn at these conditions, this is a reasonable approach of pressure determination for such experiments. The simulation showed a peak pressure in the Sn sample of 85(5) GPa. We note that, as a best practice, performing complementary experiments using a LiF window would be advisable. This would enable the measurement of Sn-LiF particle velocity histories, allowing for a more accurate determination of pressure. Therefore, the values reported here should be considered estimates. We do not measure temperature in these experiments—temperature at 85 GPa are estimated using the Sn Hugoniot from SESAME table 2162.

LASER ENERGY VS ABLATION PRESSURE

We performed a series of experiments on polyimide-LiF and polyimide-Cu targets at a range of laser energies with both 250 and $500\,\mu m$ phase plates. For a known laser energy (determined by a calorimeter placed in the path of the drive beam), the peak pressure in the polyimide was determined to construct an empirical laser energy vs ablation pressure for the DiPOLE 100-X laser (Fig. 3). In the experiments using polyimide-LiF targets (plotted using black squares in Fig. 3), the peak pressure in the polyimide was determined by using the VISAR diagnostic and impedance matching from the LiF window.[19,20]

In the experiments using polyimide-Cu targets (plotted using red filled and red open squares in Fig. 3), the Cu pressure was determined by fitting the diffraction pattern to a high-temperature EOS for Cu (Refs. 21 and 22) and corresponding polyimide pressure was determined from impedance matching. This empirical
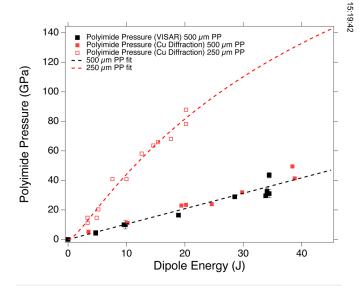

FIG. 3. Polyimide pressure as a function of laser energy for 500 and $250\,\mu m$ phase plates (PPs). This relation was determined by two independent methods: using impedance matching from VISAR traces from polyimide-LiF targets (black); using impedance matching from Cu diffraction data from polyimide-Cu targets (red).

energy vs pressure relation was found to be significantly less efficient than theoretical ablation scaling laws[23] as it was found that considerable laser energy is distributed outside of the main focal spot. This additional energy was found to potentially cause damage to adjacent targets in the holder (see the supplementary material). To overcome this issue, targets were positioned in every other hole on the holder to increase the distance from each other. Future improvements to the platform will include new phase plates that do not exhibit this issue. It is always best to determine pressure on a shot by a direct VISAR measurement to account for shot-to-shot errors in energy determination, sample alignment, sample metrology, and other variations. But, the energy vs pressure relations shown here will allow future users to design experiments for any sample of interest and predict the conditions which can be reached using the HED instrument.

X-RAY DIFFRACTION MEASUREMENTS

Experiments were performed during the #2740 experimental campaign which represented a community-wide effort and the first user experiments using the DiPOLE 100-X laser at the HED instrument. A number of materials were investigated during this campaign but here we restrict our discussion to shock-melting of elemental Sn. The Sn samples discussed here were shock-compressed and the EuXFEL pulse was timed such that each sample was probed before the shock wave had traveled through the entire sample. This meant that when probed by the EuXFEL x-ray pulse, the majority of the sample existed at a uniform high-pressure, high-temperature state with a small region ahead of the shock wave at ambient conditions. This is observed in the diffraction images, with diffraction peaks from the compressed sample appearing more broad and powder-like (or diffuse in the case of liquid scattering) compared with the sharper and more textured nature of the ambient sample (Fig. 1). The diffraction peaks from the ambient signal agreed well with those predicted from the β-Sn structure (space group symmetry I4$_1$/amd, a = 5.832 Å, c = 3.181 Å) and were masked out using the x-ray analysis package Dioptas[24] to isolate the diffraction signal arising from the compressed sample. Diffraction originating from the Al target holder was also observed in some cases and was also masked out.

The detector positions and sample detector distances are precisely calibrated using a CeO$_2$ standard with a known lattice parameter of 5.411 Å (see the supplementary material). For quantitative analysis of liquid samples, it is imperative to accurately measure the scattering intensity, especially at high diffraction angles. To ensure that the intensity of the liquid scattering is accurate, we made several corrections which included: (i) subtracting a "dark" image collected immediately before the experiment which corresponded to the average readout when no x rays were present; (ii) the linear polarization of the EuXFEL beam;[25] (iii) the self attenuation of the Sn sample, which becomes large at high diffraction angle (see the supplementary material); (iv) the absorption of the Al filter in front of the detectors, which is a function of diffraction angle [Fig. 4(a)]. The Sn target design did not use a confining LiF window but for experiments in which windows are used, their contribution to the overall scattering must be considered and subtracted. This correction may become significant for target designs

which use thick (500) μm windows and also samples of interest with low atomic number. The Al filter correction was achieved by irradiating a yttrium–aluminum–garnet (YAG) single crystal with the EuXFEL beam to induce a fluorescence signal. The isotropic nature of the fluorescence emission allows for the flat-fielding of each Varex detector on a pixel-by-pixel basis [Fig. 4(b)]. These corrections were found to be crucial to enable structural analysis of the measured liquid scattering signals. The corrected intensities from each Varex detector were summed and then the combined image was azimuthally integrated to produce a 1D line out which was used for structural analysis [Fig. 5(d)].

Liquid structure analysis

In run 826 of the experimental campaign, a Sn sample was shock-compressed to a peak pressure of 85(5) GPa (Fig. 2) and
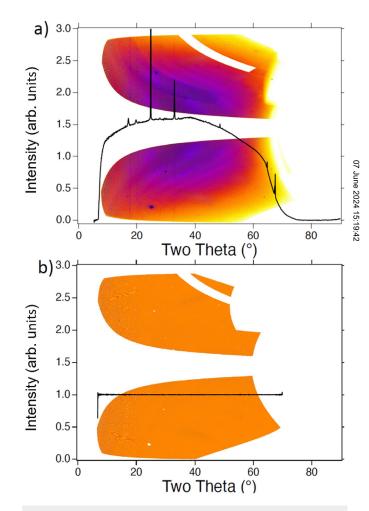

FIG. 4. Flat-fielding the Varex detectors. YAG crystal was illuminated with EuXFEL beam to induce fluorescence emission. (a) Uncorrected image from Varex detectors with accompanying line out. (b) Corrected image with parasitic Bragg reflections masked out.[24]

probed by the EuXFEL beam 1 ns before shock breakout at the rear surface. The diffraction pattern shows clear evidence of liquid scattering as the diffraction maxima are broad and diffuse in nature [Figs. 5(a) and 5(b)].

The atomic structure factor is defined as

$$S(Q) = 1 + \frac{4\pi n}{Q} \int_0^\infty [g(r) - 1] r \sin(Qr) dr, \quad (1)$$

where n is the average number density, r is the distance between atoms, and $g(r)$ is the pair distribution function. $S(Q)$ is obtained by scaling the diffracted intensity by the atomic scattering factor[26] and normalizing it to 1 at the largest experimental Q value [$Q = \frac{4\pi \sin(\theta)}{\lambda}$ where θ is the scattering angle and λ is the x-ray wavelength]. The determined structure factor is shown in Fig. 5(c). The $g(r)$ function [shown in Fig. 5(d)] is related to the probability of finding the center of an atom at a given distance from the center of a reference atom and is useful for monitoring structural changes in a liquid. The density of the liquid can be extracted by applying an optimization procedure first outlined by Eggert *et al.*[27] which minimizes a figure of merit,

$$\chi^2 = \int_0^{r_{cutoff}} [F(r) + 4\pi n]^2 dr, \quad (2)$$

where $F(r) = 4\pi n[g(r) - 1]$ and r_{cutoff} represents the minimum distance at which an atom may be located from another atom (normally equivalent to a value close to the atomic diameter). The optimization varied three parameters: (i) a constant background signal (the initial value was taken to be 0.1); (ii) the r_{cutoff} (the initial value was selected as 1.45 Å which is the atomic diameter of Sn; (iii) and n (the initial value was set at 0.0578 which is equivalent to 11.4 g/cm^3) which is the expected density of Sn shock

compressed to 85 GPa. The parameters were updated using the BOBYQA optimization algorithm[28,29] and iterations occur until a clear minimum in χ^2 is realized.

When performing liquid structure analyses, an important value is the choice of Q_{max} which defines an upper limit of Q above which, no intensity data will be considered. As $g(r)$ is a Fourier transform of $S(Q)$ an insufficiently large Q_{max} can cause non-physical oscillations at low $g(r)$, which can inhibit the success of the liquid density optimization described in Eq. (2). In contrast, a choice of Q_{max} beyond where one is confident that the intensity corrections are valid can also introduce spurious features at low $g(r)$, which can also impact the accuracy of density optimization. The experimental geometry and choice of x-ray wavelength in these experiments allowed for data to be collected up to maximum Q values of $\sim$9.5 Å^{-1}. The density optimization procedure was performed for a range of Q_{max} between 6.0 Å^{-1} and 9.1 Å^{-1} (Fig. 6). As can be seen, there is a clear minimum in the χ^2 value as a function of Q_{max} between 6.8 Å^{-1} and 8.8 Å^{-1} indicating that the optimization procedure is stable and well behaved in this range. The average density was determined to be 11.56(15) g/cm^3, which represents a 1.3% density uncertainty from a liquid Sn sample at 85 GPa and 3500 K. The coordination number, which represents the average number of nearest neighbor atoms to a reference atom, can

FIG. 6. Effect of Q_{max} on optimization—shot 826. Density and χ^2 (top) and coordination number (bottom) as determined as a function of Q_{max}. The figure of merit χ^2 (red) is minimized between 7.0 and 8.8 Å^{-1}.
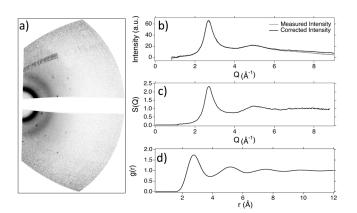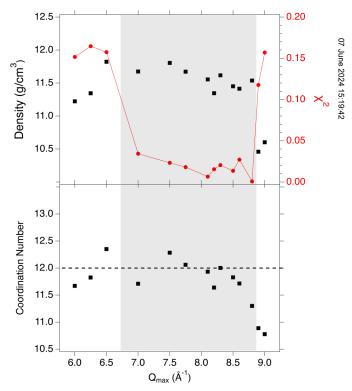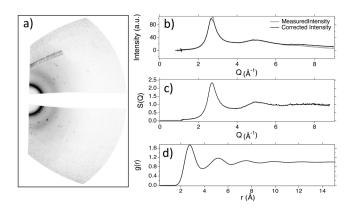
FIG. 5. Structural analysis of liquid Sn—shot 826. (a) 2D diffraction image warped into a geometric view such that diffraction rings are concentric circles. (b) 1D integrated line out from uncorrected and corrected data. (c) Optimized $S(Q)$ profile. (d) Optimized $g(r)$ profile.

FIG. 7. Structural analysis of liquid Sn—shot 831. (a) 2D diffraction image warped into a geometric view such that diffraction rings are concentric circles. (b) 1D integrated line out from uncorrected and corrected data. (c) Optimized $S(Q)$ profile. (d) Optimized $g(r)$ profile.

be expressed as

$$CN = \int_0^{r_{\min}} 4\pi n r^2 g(r) dr, \tag{3}$$

where $r_{\min}$ is the location of the minimum after the first peak in $g(r)$. The coordination number of liquid Sn as a function of $Q_{\max}$ is shown in Fig. 6 and the average value within the limit of $7.0 > Q > 8.8$ was determined to be 11.9(3) indicating that liquid Sn can be described as a simple liquid at these conditions. Indeed, QMD simulations of liquid Sn at similar conditions have reported a coordination number of 12.0.[8]

Shot 831 of the experimental campaign represented a repeat experiment of shot 826. A Sn target was again shock compressed to a peak pressure of 85(5) GPa and probed by the EuXFEL beam 0.5 ns before shock breakout at the rear surface. The diffraction pattern again showed clear evidence of liquid diffraction (Fig. 7). The density was determined from the average value of individual optimizations over a Q-range, where the figure of merit χ^2 is sufficiently minimized ($7 > Q > 8.8$) and was found to be 11.50(15) g/cm^3 and a coordination number of 11.9(2) (Fig. 8).

DISCUSSION

Our results demonstrate that high precision structural measurements are achievable using the HED instrument at the EuXFEL at conditions which are challenging to access via static compression methods. The ability to measure liquid density at extreme pressures and temperatures is promising for many scientific fields such as planetary science. For example, understanding the density of iron-bearing silicates as a function of pressure and the conditions of melting are key to modeling magma ocean dynamics of rocky planets.[30]

The experimental setup at the HED instrument overcomes previous experimental difficulties experienced at other facilities,
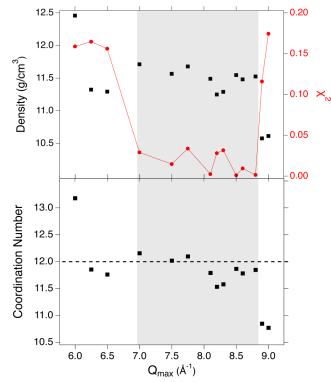

FIG. 8. Effect of $Q_{\max}$ on optimization—shot 831. Density and χ^2 (top) and coordination number (bottom) was determined as a function of $Q_{\max}$. The figure of merit χ^2 (red) is minimized between 7.0 and 8.8 Å^{-1}.

which impacted the quality of diffraction obtained. Structure factor and pair distribution profiles of shock melted Sn from different dynamic compression facilities as well as quantum molecular dynamic simulations are shown in Fig. 9. Experiments performed at the Matter in Extreme Conditions end station (MEC) of the Linac Coherent Light Source (LCLS) in 2017[7] were hindered by the limited angular coverage as well as issues surrounding the complex gain behavior of the Cornel-Stanford Pixel Array Detectors (CSPADs) which created artifacts in the $S(Q)$ data such as the feature at 6.2 Å^{-1} in Fig. 9. Since 2017, the operating x-ray energy at MEC is now up to 25 keV and there is an effort to soon field the same Varex detectors as used in the experiments reported here. Both improvements will dramatically improve the quality of liquid diffraction data obtainable at this facility. Experiments performed at the Dynamic Compression Sector (DCS) in 2021[8] had sufficient angular coverage and a robust large area detector, but used a broad, asymmetric x-ray source. While a correction was applied to these data to account for source energy asymmetry, the correction impacted the accuracy with which the density could be determined and also introduced spurious features in the $g(r)$ profiles such as the features at 3.5 and 4.5 Å in Fig. 9. The Advanced Photon Source (APS) (where DCS is situated) is currently undergoing an upgrade which will mean the x-ray source will be highly
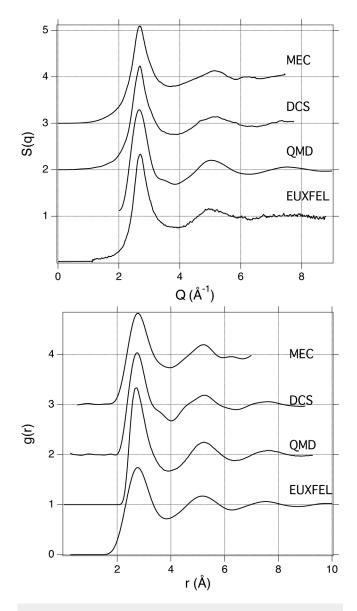
07 June 2024 15:19:42

FIG. 9. Comparison with other facilities and simulation. $S(Q)$ (a) and $g(r)$ (b) data from this work compares well with similar measurements performed at DCS and MEC as well as the results of QMD simulations performed at similar conditions. The accuracy of the measurements at MEC and DCS were hindered by experimental constraints (see text).

monochromatic thus improving the quality of liquid diffraction data obtainable at this facility. The data collected at the EuXFEL overcome these experimental difficulties with the use of large-area scintillator based detectors, a high x-ray energy (18 keV) and highly monochromatic x-ray source ($\frac{\Delta E}{E} = 0.1\%$) to achieve $S(Q)$ and $g(r)$ profiles which are in excellent agreement with those produced from QMD simulations at similar conditions.

In summary, we have demonstrated that high quality liquid diffraction measurements including novel density contrast measurements of a sample as it melts are possible using the HED instrument at the EuXFEL. Using shock compressed Sn as an example, we reported liquid density measurements with uncertainties of 1.3% at a pressure of 85(5) GPa and ∼3500 K. We have discussed the intensity corrections which are necessary for the quantitative analysis of the liquid diffraction data, as well as the methods for determining the sample pressure history. We have also provided a laser energy vs polyimide ablator pressure relations which will be useful to users planning future experiments at the facility.

SUPPLEMENTARY MATERIAL

See the supplementary material for more information on the Varex detector calibrations; the energy deposition due to the phase plates used and tabular forms of the data presented in Figs. 3, 6, and 8 from the main text.

ACKNOWLEDGMENTS

07 June 2024 15:19:42

AUTHOR DECLARATIONS

Conflict of Interest

The authors have no conflicts to disclose.

Competing Interests

The authors declare no competing interests.

Author Contributions

M. G. Gorman: Conceptualization (equal); Writing – review & editing (equal). **D. McGonegle:** Conceptualization (equal); Writing – review & editing (equal). **R. F. Smith:** Conceptualization (equal); Writing – original draft (equal); Writing – review & editing (equal). **S. Singh:** Conceptualization (equal); Software (equal); Writing – original draft (equal); Writing – review & editing (equal). **T. Jenkins:** Formal analysis (equal); Software (equal); Writing – review & editing (equal). **R. S. McWilliams:** Conceptualization (equal); Formal analysis (equal); Writing – original draft (equal); Writing – review & editing (equal). **B. Albertazzi:** Conceptualization (equal); Writing – original draft (equal); Writing – review & editing (equal). **S. J. Ali:** Conceptualization (equal); Data curation (equal); Writing – review & editing (equal). **L. Antonelli:** Conceptualization (equal); Data curation (equal); Writing – review & editing (equal). **M. R. Armstrong:** Conceptualization (equal); Writing – review & editing (equal). **C. Baehtz:** Conceptualization (equal); Writing – review & editing (equal). **O. B. Ball:** Conceptualization (equal); Resources (equal); Writing – review & editing (equal). **S. Banerjee:** Conceptualization (equal); Resources (equal); Writing – review & editing (equal). **A. B. Belonoshko:** Conceptualization (equal); Writing – review & editing (equal). **A. Benuzzi-Mounaix:** Conceptualization (equal); Writing – review & editing (equal). **C. A. Bolme:** Conceptualization (equal); Writing – review & editing (equal). **V. Bouffetier:** Conceptualization (equal); Writing – review & editing (equal). **R. Briggs:** Conceptualization (equal); Writing – review & editing (equal). **K. Buakor:** Conceptualization (equal); Writing – review & editing (equal). **T. Butcher:** Conceptualization (equal); Writing – review & editing (equal). **S. Di Dio Cafiso:** Conceptualization (equal); Writing – review & editing (equal). **V. Cerantola:** Conceptualization (equal); Writing – review & editing (equal). **J. Chantel:** Conceptualization (equal); Writing – review & editing (equal). **A. Di Cicco:** Conceptualization (equal); Writing – review & editing (equal). **S. Clarke:** Conceptualization (equal); Writing – review & editing (equal). **A. L. Coleman:** Conceptualization (equal); Writing – review & editing (equal). **J. Collier:** Conceptualization (equal); Writing – review & editing (equal). **G. W. Collins:** Conceptualization (equal); Writing – review & editing (equal). **A. J. Comley:** Conceptualization (equal); Writing – review & editing (equal). **F. Coppari:** Conceptualization (equal); Writing – review & editing (equal). **T. E. Cowan:** Conceptualization (equal); Writing – review & editing (equal). **G. Cristoforetti:** Conceptualization (equal); Writing – review & editing (equal). **H. Cynn:** Conceptualization (equal); Writing – review & editing (equal). **A. Descamps:** Conceptualization (equal); Writing – review & editing (equal). **F. Dorchies:** Conceptualization (equal); Writing – review & editing (equal). **M. J. Duff:** Conceptualization (equal); Writing – review & editing (equal). **A. Dwivedi:** Conceptualization (equal); Writing – review & editing (equal). **C. Edwards:** Conceptualization (equal); Writing – review & editing (equal). **J. H. Eggert:** Conceptualization (equal); Writing – review & editing (equal). **D. Errandonea:** Conceptualization (equal); Writing – review & editing (equal). **G. Fiquet:** Conceptualization (equal); Writing – review & editing (equal). **E. Galtier:** Conceptualization (equal); Writing – review & editing (equal). **A. Laso Garcia:** Conceptualization (equal); Writing – review & editing (equal). **H. Ginestet:** Conceptualization (equal); Writing – review & editing (equal). **L. Gizzi:** Conceptualization (equal); Writing – review & editing (equal). **A. Gleason:** Conceptualization (equal); Writing – review & editing (equal). **S. Goede:** Conceptualization (equal); Writing – review & editing (equal). **J. M. Gonzalez:** Conceptualization (equal); Writing – review & editing (equal). **M. Harmand:** Conceptualization (equal); Writing – review & editing (equal). **N. J. Hartley:** Conceptualization (equal); Writing – review & editing (equal). **P. G. Heighway:** Conceptualization (equal); Writing – review & editing (equal). **C. Hernandez-Gomez:** Conceptualization (equal); Writing – review & editing (equal). **A. Higginbotham:** Conceptualization (equal); Writing – review & editing (equal). **H. Höppner:** Conceptualization (equal); Writing – review & editing (equal). **R. J. Husband:** Conceptualization (equal); Writing – review & editing (equal). **T. M. Hutchinson:** Conceptualization (equal); Writing – review & editing (equal). **H. Hwang:** Conceptualization (equal); Writing – review & editing (equal). **A. E. Jenei:** Conceptualization (equal); Writing – review & editing (equal). **D. A. Keen:** Conceptualization (equal); Writing – review & editing (equal). **J. Kim:** Conceptualization (equal); Writing – review & editing (equal). **P. Koester:** Conceptualization (equal); Writing – review & editing (equal). **Z. Konopkova:** Conceptualization (equal); Writing – review &

07 June 2024 15:19:42

editing (equal). **D. Kraus:** Conceptualization (equal); Writing – review & editing (equal). **A. Krygier:** Conceptualization (equal); Writing – review & editing (equal). **L. Labate:** Conceptualization (equal); Writing – review & editing (equal). **Y. Lee:** Conceptualization (equal); Writing – review & editing (equal). **H.-P. Liermann:** Conceptualization (equal); Writing – review & editing (equal). **P. Mason:** Conceptualization (equal); Writing – review & editing (equal). **M. Masruri:** Conceptualization (equal); Writing – review & editing (equal). **B. Massani:** Conceptualization (equal); Writing – review & editing (equal). **E. E. McBride:** Conceptualization (equal); Writing – review & editing (equal). **C. McGuire:** Conceptualization (equal); Writing – review & editing (equal). **J. D. McHardy:** Conceptualization (equal); Writing – review & editing (equal). **S. Merkel:** Conceptualization (equal); Writing – review & editing (equal). **G. Morard:** Conceptualization (equal); Writing – review & editing (equal). **B. Nagler:** Conceptualization (equal); Writing – review & editing (equal). **M. Nakatsutsumi:** Conceptualization (equal); Writing – review & editing (equal). **K. Nguyen-Cong:** Conceptualization (equal); Writing – review & editing (equal). **A.-M. Norton:** Conceptualization (equal); Writing – review & editing (equal). **I. I. Oleynik:** Conceptualization (equal); Writing – review & editing (equal). **C. Otzen:** Conceptualization (equal); Writing – review & editing (equal). **N. Ozaki:** Conceptualization (equal); Writing – review & editing (equal). **S. Pandolfi:** Conceptualization (equal); Writing – review & editing (equal). **D. J. Peake:** Conceptualization (equal); Writing – review & editing (equal). **A. Pelka:** Conceptualization (equal); Writing – review & editing (equal). **K. A. Pereira:** Conceptualization (equal); Writing – review & editing (equal). **J. P. Phillips:** Conceptualization (equal); Writing – review & editing (equal). **C. Prescher:** Conceptualization (equal); Writing – review & editing (equal). **T. R. Preston:** Conceptualization (equal); Writing – review & editing (equal). **L. Randolph:** Conceptualization (equal); Writing – review & editing (equal). **D. Ranjan:** Conceptualization (equal); Writing – review & editing (equal). **A. Ravasio:** Conceptualization (equal); Writing – review & editing (equal). **R. Redmer:** Conceptualization (equal); Writing – review & editing (equal). **J. Rips:** Conceptualization (equal); Writing – review & editing (equal). **D. Santamaria-Perez:** Conceptualization (equal); Writing – review & editing (equal). **D. J. Savage:** Conceptualization (equal); Writing – review & editing (equal). **M. Schoelmerich:** Conceptualization (equal); Writing – review & editing (equal). **J.-P. Schwinkendorf:** Conceptualization (equal); Writing – review & editing (equal). **J. Smith:** Conceptualization (equal); Writing – review & editing (equal). **A. Sollier:** Conceptualization (equal); Writing – review & editing (equal). **J. Spear:** Conceptualization (equal); Writing – review & editing (equal). **C. Spindloe:** Conceptualization (equal); Writing – review & editing (equal). **M. Stevenson:** Conceptualization (equal); Writing – review & editing (equal). **C. Strohm:** Conceptualization (equal); Writing – review & editing (equal). **T.-A. Suer:** Conceptualization (equal); Writing – review & editing (equal). **M. Tang:** Conceptualization (equal); Writing – review & editing (equal). **M. Toncian:** Conceptualization (equal); Writing – original draft (equal); Writing – review & editing (equal). **T. Toncian:** Conceptualization (equal); Writing – review & editing (equal). **S. J. Tracy:** Conceptualization (equal); Writing – review & editing (equal). **A. Trapananti:** Conceptualization (equal); Writing – review & editing (equal). **T. Tschentscher:** Conceptualization (equal); Writing – review & editing (equal). **M. Tyldesley:** Conceptualization (equal); Writing – review & editing (equal). **C. E. Vennari:** Conceptualization (equal); Writing – review & editing (equal). **T. Vinci:** Conceptualization (equal); Writing – review & editing (equal). **S. C. Vogel:** Conceptualization (equal); Writing – review & editing (equal). **T. J. Volz:** Conceptualization (equal); Writing – review & editing (equal). **J. Vorberger:** Conceptualization (equal); Writing – review & editing (equal). **J. P. S. Walsh:** Conceptualization (equal); Writing – review & editing (equal). **J. S. Wark:** Conceptualization (equal); Writing – review & editing (equal). **J. T. Willman:** Conceptualization (equal); Writing – review & editing (equal). **L. Wollenweber:** Conceptualization (equal); Writing – review & editing (equal). **U. Zastrau:** Conceptualization (equal); Writing – review & editing (equal). **E. Brambrink:** Conceptualization (equal); Writing – review & editing (equal). **K. Appel:** Conceptualization (equal); Writing – review & editing (equal). **M. I. McMahon:** Conceptualization (equal); Writing – review & editing (equal).

DATA AVAILABILITY

Data recorded for the experiment at the European XFEL are available at doi:10.22003/XFEL.EU-DATA-002740-00. The corresponding run numbers and calibration for the x-ray diffraction data processing are provided in the supplementary material.

REFERENCES

[1]R. Briggs, M. Gorman, A. Coleman, R. McWilliams, E. McBride, D. McGonegle, J. Wark, L. Peacock, S. Rothman, S. Macleod, and C. A. Bolme, "Ultrafast x-ray diffraction studies of the phase transitions and equation of state of scandium shock compressed to 82 GPa," Phys. Rev. Lett. **118**, 025501 (2017).

[2]A. Coleman, M. Gorman, R. Briggs, R. McWilliams, D. McGonegle, C. Bolme, A. Gleason, D. Fratanduono, R. Smith, E. Galtier, and H. J. Lee, "Identification of phase transitions and metastability in dynamically compressed antimony using ultrafast x-ray diffraction," Phys. Rev. Lett. **122**, 255704 (2019).

[3]D. Kraus, J. Vorberger, A. Pak, N. Hartley, L. Fletcher, S. Frydrych, E. Galtier, E. Gamboa, D. O. Gericke, S. Glenzer, and E. Granados, "Formation of diamonds in laser-compressed hydrocarbons at planetary interior conditions," Nat. Astron. **1**, 606–611 (2017).

[4]Z. He, M. Rodel, J. Lutgert, A. Bergermann, M. Bethkenhagen, D. Chekrygina, T. E. Cowan, A. Descamps, M. French, E. Galtier, and A. E. Gleason, "Diamond formation kinetics in shock-compressed C-H-O samples recorded by small-angle x-ray scattering and x-ray diffraction," Sci. Adv. **8**, eabo0617 (2022).

[5]C. E. Wehrenberg, D. McGonegle, C. Bolme, A. Higginbotham, A. Lazicki, H. J. Lee, B. Nagler, H.-S. Park, B. A. Remington, R. Rudd, and M. Sliwa, "_In situ_ x-ray diffraction measurement of shock-wave-driven twinning and lattice dynamics," Nature **550**, 496–499 (2017).

[6]M. Gorman, A. Coleman, R. Briggs, R. McWilliams, D. McGonegle, C. Bolme, A. Gleason, E. Galtier, H. Lee, E. Granados, and M. Śliwa, "Femtosecond diffraction studies of solid and liquid phase changes in shock-compressed bismuth," Sci. Rep. **8**, 16927 (2018).

[7]R. Briggs, M. Gorman, S. Zhang, D. McGonegle, A. Coleman, F. Coppari, M. Morales-Silva, R. Smith, J. Wicks, C. Bolme, and A. E. Gleason, "Coordination changes in liquid tin under shock compression determined using _in situ_ femtosecond x-ray diffraction," Appl. Phys. Lett. **115**, 264101 (2019).

[8]S. Singh, A. L. Coleman, S. Zhang, F. Coppari, M. G. Gorman, R. F. Smith, J. H. Eggert, R. Briggs, and D. E. Fratanduono, "Quantitative analysis of diffraction by liquids using a pink-spectrum x-ray source," J. Synchrotron Radiat. **29**, 1033–1042 (2022).

[9]A. L. Coleman, S. Singh, C. E. Vennari, R. F. Smith, T. J. Volz, M. G. Gorman, S. M. Clarke, J. H. Eggert, F. Coppari, D. E. Fratanduono, and R. Briggs, "Quantitative measurements of density in shock-compressed silver up to 330 GPa using x-ray diffraction," J. Appl. Phys. **131**, 015901 (2022).

[10]S. Anzellini and S. Boccato, "A practical review of the laser-heated diamond anvil cell for university laboratories and synchrotron applications," Crystals **10**, 459 (2020).

[11]S. Singh, R. Briggs, M. G. Gorman, L. X. Benedict, C. J. Wu, A. L. Coleman, F. Coppari, A. Fernandez-Panella, C. McGuire, and M. Sims, "A structural study of HCP and liquid iron under shock compression up to 275 GPa," arXiv:2304. 07933(2023).

[12]U. Zastrau, K. Appel, C. Baehtz, O. Baehr, L. Batchelor, A. Berghäuser, M. Banjafar, E. Brambrink, V. Cerantola, T. E. Cowan, and H. Damker, "The high energy density scientific instrument at the European XFEL," J. Synchrotron Radiat. **28**, 1393–1416 (2021).

[13]P. Avery, B. Major, S. Soderlind, K. Nygren, P. Shade, and J. Bernier, "Hexrd/hexrdgui: Release 1.0.0" (2023).

[14]P. Mason, S. Banerjee, J. Smith, T. Butcher, J. Phillips, H. Höppner, D. Möller, K. Ertel, M. De Vido, I. Hollingham, and A. Norton, "Development of a 100 J, 10 Hz laser for compression experiments at the high energy density instrument at the European XFEL," High Power Laser Sci. Eng. **6**, e65 (2018).

[15]P. M. Celliers, D. K. Bradley, G. W. Collins, D. G. Hicks, T. R. Boehly, and W. J. Armstrong, "Line-imaging velocimeter for shock diagnostics at the OMEGA laser facility," Rev. Sci. Instrum. **75**, 4916–4929 (2004).

[16]L. Kirsch, S. Ali, D. Fratanduono, R. Kraus, D. Braun, A. Fernandez-Pañella, R. Smith, J. McNaney, and J. Eggert, "Refractive index of lithium fluoride to 900 gigapascal and implications for dynamic equation of state measurements," J. Appl. Phys. **125**, 175901 (2019).

[17]S. Pascarelli, M. McMahon, C. Pépin, O. Mathon, R. F. Smith, W. L. Mao, H.-P. Liermann, and P. Loubeyre, "Materials under extreme conditions using large x-ray facilities," Nat. Rev. Methods Primers **3**, 82 (2023).

[18]J. T. Larsen and S. M. Lane, "HYADES—A plasma hydrodynamics code for dense plasma studies," J. Quant. Spectrosc. Radiat. Transfer **51**, 179–186 (1994).

[19]P. Celliers, G. Collins, D. Hicks, and J. Eggert, "Systematic uncertainties in shock-wave impedance-match analysis and the high-pressure equation of state of Al," J. Appl. Phys. **98**, 113529 (2005).

[20]G. I. Kerley, "Calculation of release adiabats and shock impedance matching," arXiv:1306.6913 (2013).

[21]T. S. Sokolova, P. I. Dorogokupets, A. M. Dymshits, B. S. Danilov, and K. D. Litasov, "Microsoft excel spreadsheets for calculation of P–V–T relations and thermodynamic properties from equations of state of MgO, diamond and nine metals as pressure markers in high-pressure and high-temperature experiments," Comput. Geosci. **94**, 162–169 (2016).

[22]J. D. McHardy, C. V. Storm, M. J. Duff, S. G. Macleod, and M. I. McMahon, "On the creation of thermal equations of state for use in DIOPTAS," High Pressure Res. **43**, 40–57 (2023).

[23]R. P. Drake and R. P. Drake, *Introduction to High-Energy-Density Physics* (Springer, 2006).

[24]C. Prescher and V. B. Prakapenka, "DIOPTAS: A program for reduction of two-dimensional x-ray diffraction data and data exploration," High Pressure Res. **35**, 223–230 (2015).

[25]K. S. Schulze, B. Grabiger, R. Loetzsch, B. Marx-Glowna, A. T. Schmitt, A. L. Garcia, W. Hippler, L. Huang, F. Karbstein, Z. Konôpková, and H. P. Schlenvoigt, "Towards perfectly linearly polarized x-rays," Phys. Rev. Res. **4**, 013220 (2022).

[26]J. H. Hubbell, W. J. Veigele, E. Briggs, R. Brown, D. Cromer, and D. R. Howerton, "Atomic form factors, incoherent scattering functions, and photon scattering cross sections," J. Phys. Chem. Ref. Data **4**, 471–538 (1975).

[27]J. H. Eggert, G. Weck, P. Loubeyre, and M. Mezouar, "Quantitative structure factor and density measurements of high-pressure fluids in diamond anvil cells by x-ray diffraction: Argon and water," Phys. Rev. B **65**, 174105 (2002).

[28]M. J. Powell, "The BOBYQA algorithm for bound constrained optimization without derivatives," Cambridge NA Report NA2009/06, University of Cambridge, Cambridge **26** (2009).

[29]C. Cartis, J. Fiala, B. Marteau, and L. Roberts, "Improving the flexibility and robustness of model-based derivative-free optimization solvers," ACM Trans. Math. Softw. (TOMS) **45**, 1–41 (2019).

[30]R. Caracas, K. Hirose, R. Nomura, and M. D. Ballmer, "Melt-crystal density crossover in a deep magma ocean," Earth Planet. Sci. Lett. **516**, 202–211 (2019).

07 June 2024 15:19:42